Frontiers of Information Technology & Electronic Engineering
www.jzus.zju.edu.cn; engineering.cae.cn; www.springerlink.com
ISSN 2095-9184 (print); ISSN 2095-9230 (online)
E-mail: jzus@zju.edu.cn

Review:

Mutual coupling reduction of multiple antenna systems*

Jia-yin GUO[1], Feng LIU[1], Guo-dong JING[1], Lu-yu ZHAO[†‡1], Ying-zeng YIN[1], Guan-long HUANG[2]

[1]*Key Laboratory of Antennas and Microwave Technologies, Xidian University, Xi'an 710071, China*

[2]*Guangdong Provincial Mobile Terminal Microwave and Millimeter-Wave Antenna Engineering Research Center, College of Information Engineering, Shenzhen University, Shenzhen 518060, China*

[†]E-mail: lyzhao@xidian.edu.cn

Received Sept. 11, 2019; Revision accepted Dec. 27, 2019; Crosschecked Feb. 24, 2020

Abstract: A multi-band multi-antenna system has become an important trend in the development of mobile communication systems. However, strong mutual coupling tends to occur between antenna elements with a small space, distorting array antennas' performance. Therefore, in the multiple-input multiple-output (MIMO) antenna system, high isolation based on miniaturization of the antenna array has been pursued. We study in depth the methods of decoupling between antenna elements. Reasons for the existence of mutual coupling and advantages of mutual coupling reduction are analyzed. Then the decoupling methods proposed in recent works are compared and analyzed. Finally, we propose a metasurface consisting of double-layer short wires, which can be applied to improve the port isolation of antennas arranged along the H-plane and E-plane. Results show that the proposed metasurface has good decoupling effect on a closely placed antenna array.

Key words: Mutual coupling; Multiple-input multiple-output; Antenna array; Metasurface; Decoupling
https://doi.org/10.1631/FITEE.1900490 **CLC number:** TN82

1 Introduction

With the rapid development of wireless communication systems, high quality and long distance have become inevitable trends. Improving communication capacity and reliability has become the primary issue to be solved in the development of communication technology. Multiple-input multiple-output (MIMO) technology can achieve stable and high-speed information transmission over a long distance, so it has been studied extensively. MIMO technology can significantly improve channel capacity and transmission reliability without increasing transmission bandwidth or power (Feng et al., 2013; Larsson et al., 2014; Jafri et al., 2016). Research on MIMO antennas, a key element of communication systems, directly affects communication systems' quality and distance.

In recent years, with the development of integrated circuits, the integration of wireless terminal modules has expanded, reducing the size of radio frequency receiving and transmitting devices. Therefore, the communication system antenna must be small. MIMO antenna miniaturization is now a mainstream trend. Generally, when designing an antenna array, the space between antenna elements must be at least $\lambda_0/2$ to ensure good performance. Balancing compactness with performance is the key to designing a MIMO antenna array (Browne et al., 2006; Chae et al., 2007; Li JF et al., 2013). Placing multiple antennas in a limited space results in a strong coupling between antenna elements. The smaller the antenna element space, the stronger the mutual coupling. This mutual coupling will cause the antenna elements' current to change, which will deteriorate the antenna's performance. The mutual coupling of the antenna is shown in Fig. 1, including the transmitting and receiving antenna arrays.

‡ Corresponding author
* Project supported by the National Natural Science Foundation of China (No. 61701366)
ORCID: Jia-yin GUO, https://orcid.org/0000-0001-6963-8617; Lu-yu ZHAO, https://orcid.org/0000-0001-8981-9829

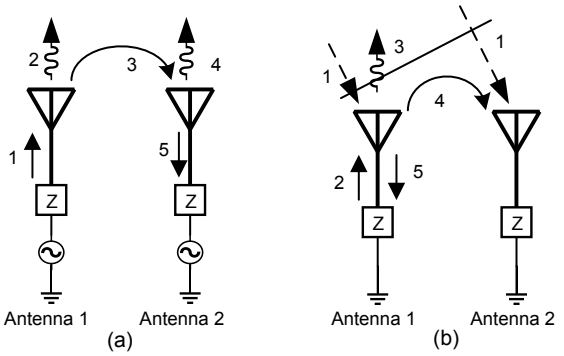

Fig. 1 Mutual coupling of antenna arrays: (a) transmitting antenna array; (b) receiving antenna array

In Fig. 1a, when antenna 1 is excited to generate electromagnetic waves, a part of energy 2 is directly radiated into free space, and another part of energy 3 is coupled into the adjacent antenna 2. After receiving energy, antenna 2 generates current and radiates a part of energy 4 into space again. Another part of antenna 2's energy 5 enters the signal source and is superimposed with the energy generated by antenna 2, which causes the antenna to be mismatched, thereby deteriorating the antenna array's performance. Fig. 1b depicts the mutual coupling principle of the receiving antenna array, which is a process similar to that of the transmitting antenna array.

The mutual coupling of antennas will change the input impedance of antenna elements, thus causing mismatch in the antenna array. Only well-matched antennas can better radiate energy into free space. If antennas are not matched, this causes power reflection to the source, resulting in power loss. At the same time, mutual coupling will cause radiation pattern distortion, low radiation efficiency, and increased correlation between MIMO antenna elements (Getu and Andersen, 2005; Soltani and Murch, 2015).

Therefore, it becomes very important to reduce the mutual coupling between antennas and improve the array antenna's performance. Isolation, an important indicator of antenna performance, is a parameter that must be considered when designing an antenna array.

2 Discussion of decoupling methods

Decoupling of MIMO antennas has always been a hot and important research topic. To suppress the electromagnetic coupling energy between MIMO antennas and improve the MIMO antenna's efficiency based on antenna miniaturization, different types of decoupling methods have been studied. By analyzing the literature, the MIMO antennas' decoupling methods can be divided into several categories.

2.1 Decoupling networks

Decoupling networks are generally applicable to the case where antenna element space is relatively close. Decoupling networks and antennas are designed separately and independently. Decoupling networks can be further divided into three subcategories according to different forms.

2.1.1 Lumped element

A pair of monopole MIMO antennas resonant at 2.45 GHz was proposed (Chen et al., 2008). As shown in Fig. 2, the antenna's port isolation can be improved from 3 dB to more than 20 dB after a lumped reactance component is connected in parallel between the two ports.

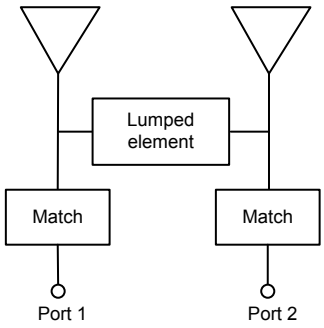

Fig. 2 Models using lumped elements for decoupling

2.1.2 Coupled resonator

The method of decoupling with a coupled resonator is based on the admittance parameters of the antenna system (Zhao LY and Wu, 2015). A pair of asymmetric and two-element antenna arrays has strong mutual coupling effects due to the small antenna space (Zhao LY et al., 2014), as shown in Fig. 3. Through the coupled resonator design, the antenna isolation can be increased to more than 20 dB under the premise of good matching.

2.1.3 Neutralization lines

The neutralization line decoupling method introduces one microstrip line or more microstrip lines between antenna elements to form a new coupling

path (Su et al., 2012; Amjadi and Sarabandi, 2016), as shown in Fig. 4. The coupling on the new coupling path can cancel the coupling between the original antennas, thereby reducing mutual coupling.

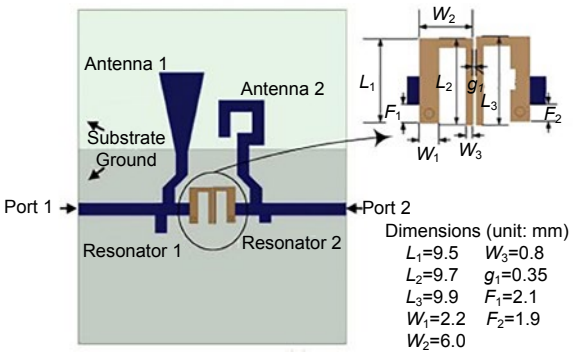

Fig. 3 Models decoupled with coupled resonators
Reprinted from Zhao LY et al. (2014), Copyright 2014, with permission from IEEE

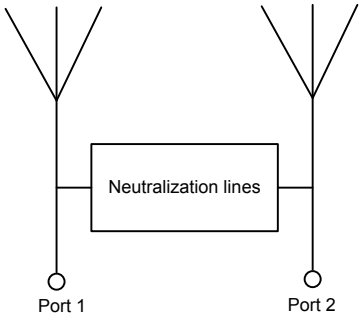

Fig. 4 Models with neutralization lines for decoupling

A broadband neutralization line structure has been proposed to reduce mutual coupling in a compact ultra-wide band (UWB) antenna system (Zhang S and Pedersen, 2016). The introduction of broadband neutralization lines can increase isolation by 12–25 dB within the working bandwidth of 3–5 GHz of the antenna.

2.2 Parasitic resonant unit

The decoupling method using a parasitic resonant unit is to introduce a coupled parasitic element between antenna elements to create an additional coupling path (Fig. 5), which uses the inverse cancellation principle of the field to improve isolation between antenna elements (Zhang Y et al., 2016; Sun et al., 2019). There are many forms of parasitic elements, such as monopole structure (Li ZY et al., 2012), mushroom structure (Zhai et al., 2016), planar inverted-F antenna (PIFA) structure (Zhao LY and Wu, 2014), split resonant ring structure (Xue et al., 2017), and ring resonator structure (Dhevi et al., 2018).

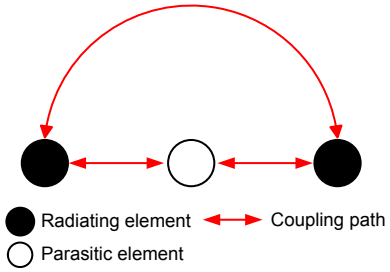

Fig. 5 Models using a parasitic element for decoupling

A decoupling method using an open resonant ring structure was proposed (Xue et al., 2017). The split resonant ring has both inductive and capacitive characteristics. The antenna's port isolation can be increased significantly in the working bandwidth after loading the split resonant ring between two antennas, which effectively reduces mutual coupling.

The parasitic structure can be not only in the same plane as the antenna, but also above the antenna, such as the array antenna decoupling surface (ADS) (Wu et al., 2017). As shown in Fig. 6, the ADS is a thin surface composed of a number of small electrical metal patches placed above the array antenna. The ADS can generate partially reflected electromagnetic waves to eliminate coupling waves from adjacent antenna elements.

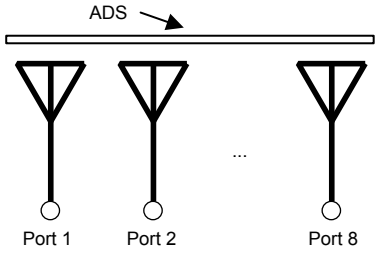

Fig. 6 Models with the antenna decoupling surface (ADS) for decoupling

2.3 Defected ground structures

Decoupling with defected ground structures is used to etch periodic or non-periodic structures on the ground of the antenna. These structures have band-stop filtering characteristics, thus changing the microwave transmission characteristics to achieve decoupling design. Decoupling with defected ground

structures can be applied to different forms of antennas, such as PIFA antennas (Zhang S et al., 2012), microstrip patch antennas (Ouyang et al., 2011), and UWB antennas (Li Q et al., 2015). Moreover, there are many forms of defected ground structures, such as periodic structures (Chiu et al., 2007), fractal structures (Wei et al., 2016), and symmetric structures (Chiu et al., 2018).

A simple rectangular slot is etched on the ground between two microstrip patch antennas to reduce the mutual coupling between two antennas (Ouyang et al., 2011), as shown in Fig. 7. The antenna isolation can be increased to more than 40 dB in the operating frequency band by etching a half-wavelength rectangular slot on the ground.

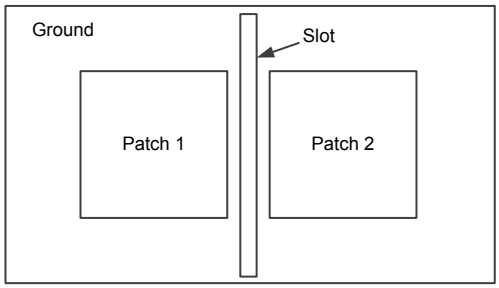

Fig. 7 Models with a rectangular slot for decoupling

Wei et al. (2016) proposed a novel fractal defected ground structure (FDGS), which uses band-stop filtering characteristics to achieve coupling suppression. The proposed structure exhibits good band-stop characteristics in the antenna's operating band by etching the third iterative FDGS.

The decoupling method based on defected ground structure is a simple and effective method to improve the isolation between antenna elements. However, the defected ground structures will affect the antenna's radiation characteristics due to the resonance characteristics. Moreover, the defected ground structures have certain antenna volume requirements that are not conducive to miniaturization design.

2.4 Pattern diversity and mode diversity

The pattern diversity method increases isolation between antenna elements and improves the radiation pattern by properly designing the antenna, so the main lobe of the antenna radiates in different directions (Liang and Wu, 2018; Zhao X et al., 2018). Pattern diversity and isolation improvement are achieved by changing the antenna's electrical length to control the pattern's radiation direction (Ding et al., 2018), as shown in Fig. 8. Based on this, the pattern diversity method with four and eight antenna elements is proposed in this study, making the isolation between antennas higher than 15 dB in the operating bandwidth.

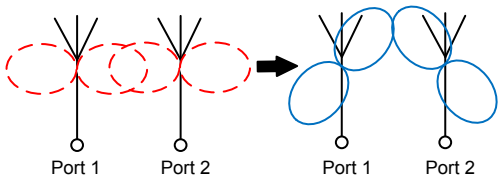

Fig. 8 Schematic of pattern diversity

Decoupled antennas based on mode analysis can achieve large isolation improvement and good antenna performance, but antenna mode design is vulnerable to the influence of antenna shell feedline and other factors. So, when antennas are decoupled in this way, these modes must be carefully designed to achieve the desired results.

2.5 Metamaterial

Recently, metamaterial decoupling has attracted wide research attention, and many decoupling methods based on it have been studied (Al-Hasan et al., 2015; Lee et al., 2015; Akbari et al., 2017; Farahani et al., 2017; Tang et al., 2017). These methods include electromagnetic band-gap (EBG) based decoupling, spoof surface plasmon polariton (SSPP) based decoupling, frequency selected surface (FSS) based decoupling, and metasurface based decoupling.

2.5.1 Electromagnetic band-gap based decoupling

Decoupling using the EBG structure has been first proposed by Yang and Rahmat-Samii (2003), and the near-field distribution of the EBG structure proves that it has good surface wave suppression characteristics. Therefore, as shown in Fig. 9, introducing the EBG structure between antenna elements can effectively reduce mutual coupling.

The EBG structure can effectively suppress surface wave propagation and achieve high-isolation characteristics of the antenna. However, it requires a certain space between antenna elements, which increases the antenna array's overall size.

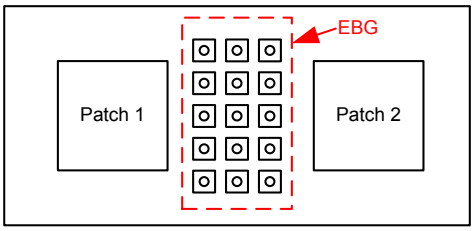

Fig. 9 Models with electromagnetic band-gap (EBG) for decoupling

2.5.2 Spoof surface plasmon polariton based decoupling

A decoupling method for a dual-band microstrip antenna (MSA), proposed by Pan and Cui (2017), is based on two transmission lines, including a substrate integrated waveguide (SIW) and an SSPP. The proposed method can achieve broadband isolation between two ports of the MSA without occupying extra space due to the low-pass characteristics of SIW and the high-pass characteristics of SSPP.

2.5.3 Frequency selected surface based decoupling

Zhu et al. (2019) proposed a method to improve the isolation of a dual-band base station antenna system based on an FSS. As shown in Fig. 10, a dual-polarized dipole antenna operating in the B1 band (0.69–0.96 GHz) and a 2×2 antenna array operating in the B2 band (3.5–4.9 GHz) are placed in a common aperture. However, the high-frequency antenna's radiation performance deteriorates significantly due to the mutual coupling effects from the low-frequency antenna. Thus, as shown in Fig. 11, an FSS composed of a metal square ring is added between the high- and low-frequency antennas to reduce coupling. According to the results in Zhu et al. (2019), the radiation patterns of antennas tend to be stable in both frequency bands, indicating that the FSS effectively suppresses the mutual coupling between the dual-band antennas.

2.5.4 Metasurface based decoupling

A decoupling method based on the split ring resonator (SRR) placed over the antenna was proposed by Wang et al. (2018) (Fig. 12). The proposed antenna metasurface has a negative permeability near the resonant frequency (5.8 GHz), and the electromagnetic wave does not propagate along the medium with this permeability. So, the mutual coupling in the MIMO antenna system can be significantly reduced.

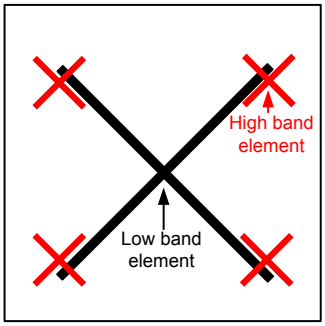

Fig. 10 Common aperture dual-band base station antenna

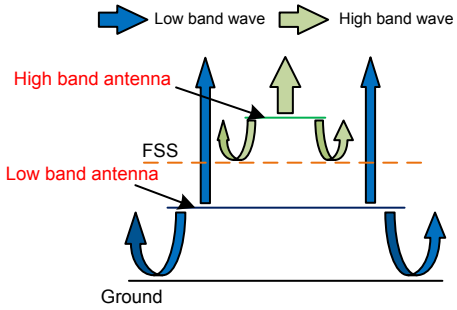

Fig. 11 Operating principle of the frequency selected surface (FSS)

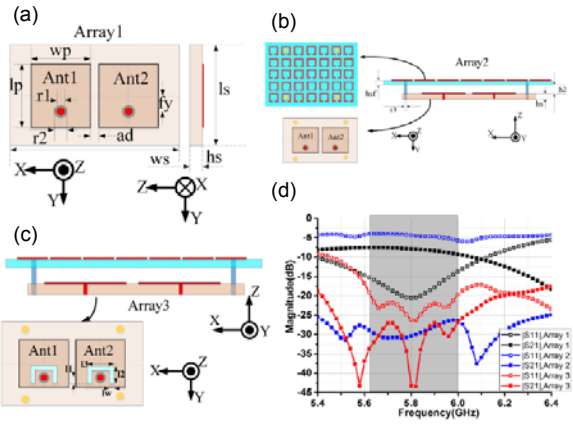

Fig. 12 Antenna model decoupled with the split ring resonator and the simulation results of *S* parameters: (a) top view (left) and side view (right) of the two-element patch array 1; (b) top view (left) and side view (right) of the two-element patch array 2 with a metasurface; (c) side view (top) and top view (bottom) of the improved two-element patch array 3 with a metasurface; (d) simulated *S* parameters of arrays 1–3

3 Discussion of decoupling methods

3.1 Antenna array coupled in the H-plane

Based on the analysis of the decoupling methods mentioned above, some decoupling designs for the antenna array have been studied with good results. In this subsection, we introduce a method for reducing mutual coupling between antenna elements with a metasurface (Liu et al., 2018). As shown in Fig. 13, by loading the metasurface over the antenna array, the direction of propagation of electromagnetic waves generated by the antenna can be changed, so many electromagnetic waves can propagate over the antenna instead of being coupled to adjacent antennas.

The antenna array coupled in the H-plane and the decoupled metasurface are shown in Fig. 14. The metasurface is composed of pairs of cut wires, which are printed on the F4B substrate with a height of 0.8 mm, a relative dielectric constant of 2.65, and a loss tangent of 0.002. The bowtie antennas and the feed structure are fabricated on the FR4 substrate with a height of 1 mm. Meanwhile, to show the metasurface's decoupling effect, a coupled antenna without metasurface is simulated and analyzed as a reference.

The measured *S* parameters of the antenna arrays with and without the metasurface (decoupled and coupled, respectively) are depicted in Fig. 15. The decoupled and coupled antenna arrays both resonate at 2.5 GHz, while the operating bandwidth of both the antennas covers 2300–2690 MHz. However, after loading the proposed metasurface, the isolation of the antenna array can be improved from about 10 dB to more than 25 dB in the operating band, which proves

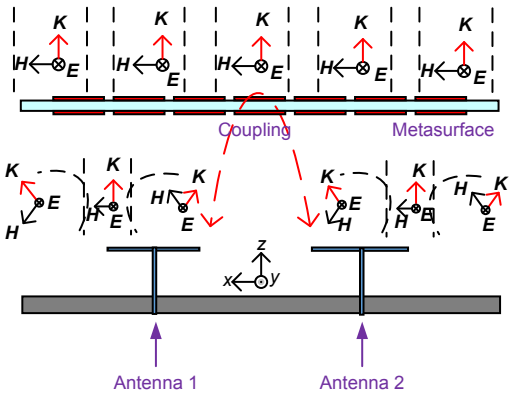

Fig. 13 Decoupling principle of the array antenna
Reprinted from Liu et al. (2018), Copyright 2018, with permission from IEEE

that the proposed metasurface has good decoupling effect.

Fig. 16 depicts the magnitude distribution of the electric field of the antenna array with and without metasurface. When the metasurface is loaded, the electric field energy is trapped around, rather than being coupled to adjacent antennas, thus improving the port isolation of the antenna array.

The measured radiation patterns of antenna arrays (coupled and decoupled) at 2.5 GHz are displayed in Fig. 17. Compared with the coupled antenna array, the peak gain of the decoupled antenna increases by about 2.5 dB. Fig. 18 shows that the total efficiency of the decoupled antenna increases by 10% in the operating band, and that the envelope correlation coefficient (ECC) reduces from 0.35 of the coupled antenna to 0.13 of the decoupled antenna. The ECC can be calculated by Eqs. (1) and (2) (see p.373).

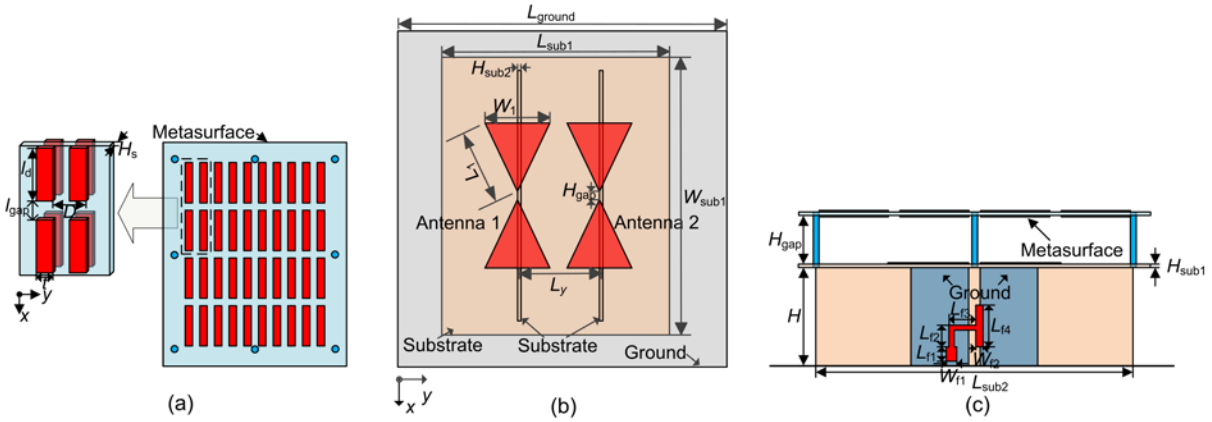

Fig. 14 Top view of the metasurface (a), two bowtie antennas (b), and side view of the two bowtie antennas (c)
Reprinted from Liu et al. (2018), Copyright 2018, with permission from IEEE

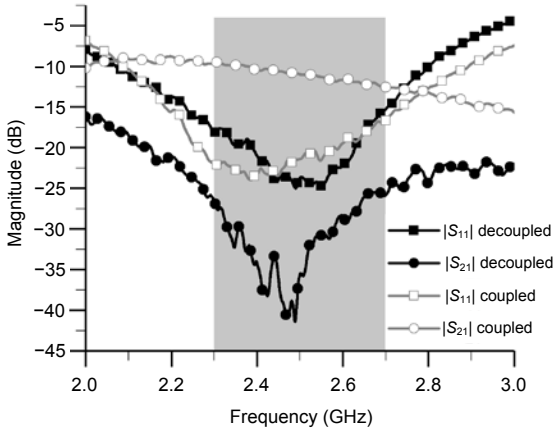

Fig. 15 Measured *S* parameters of the antenna arrays with and without metasurface
Reprinted from Liu et al. (2018), Copyright 2018, with permission from IEEE

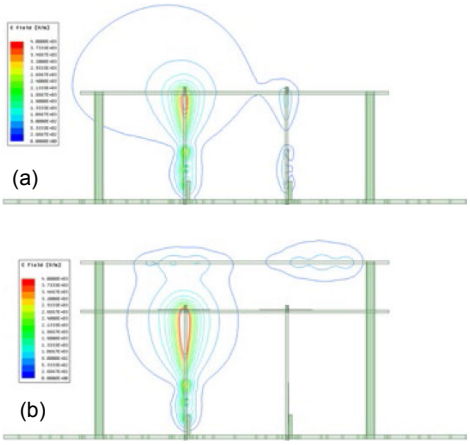

Fig. 16 Simulated magnitude distributions of the electric field for antenna arrays: (a) without metasurface; (b) with metasurface
Reprinted from Liu et al. (2018), Copyright 2018, with permission from IEEE

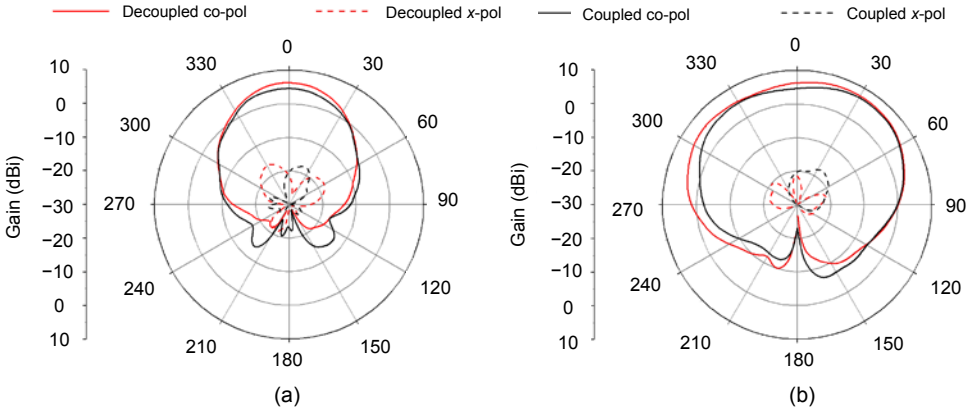

Fig. 17 Measured radiation patterns of antenna arrays at 2.5 GHz: (a) *xoz* plane; (b) *yoz* plane
Reprinted from Liu et al. (2018), Copyright 2018, with permission from IEEE

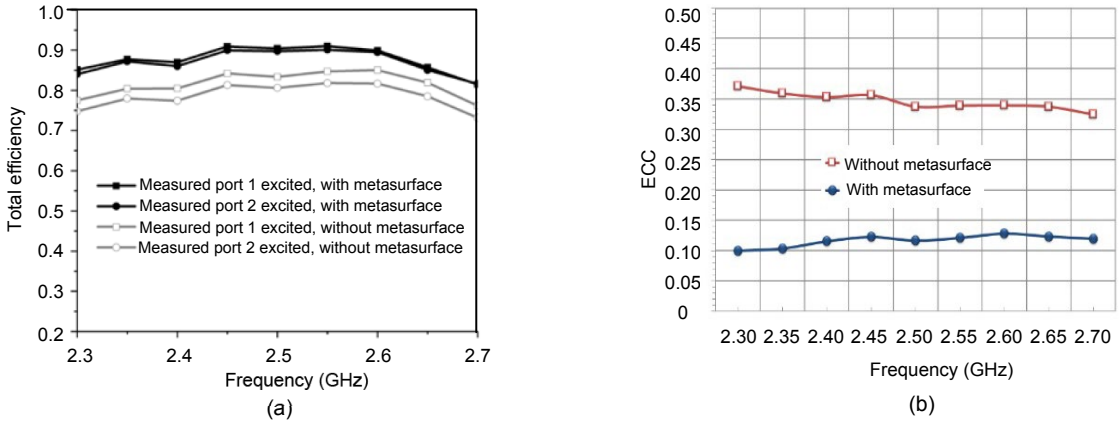

Fig. 18 Total measured efficiency (a) and calculated envelope correlation coefficient (ECC) (b) of two antenna arrays coupled in the H-plane without and with metasurface
Reprinted from Liu et al. (2018), Copyright 2018, with permission from IEEE

$$\rho_{\mathrm{e}}=\frac{\left|\iint_{4\pi}\boldsymbol{E}_1(\theta,\phi)\boldsymbol{E}_2(\theta,\phi)\mathrm{d}\Omega\right|^2}{\iint_{4\pi}|\boldsymbol{E}_1(\theta,\phi)|^2\,\mathrm{d}\Omega\iint_{4\pi}|\boldsymbol{E}_2(\theta,\phi)|^2\,\mathrm{d}\Omega},\quad(1)$$

$$\begin{aligned}\boldsymbol{E}_1(\theta,\phi)\boldsymbol{E}_2(\theta,\phi)=&E_{\theta1}(\theta,\phi)E^*_{\theta2}(\theta,\phi)\\&+E_{\phi1}(\theta,\phi)E^*_{\phi2}(\theta,\phi).\end{aligned}\quad(2)$$

3.2 Antenna array coupled in the E-plane

The base station antenna arrays in practical applications will be arranged along not only the H-plane, but also the E-plane (Guo et al., 2019). Therefore, in this subsection, we study the decoupling design for antenna arrays coupled in the E-plane. As shown in Fig. 19, two square ring-shaped dipole (SRD) antennas are arranged along the E-plane. The metasurface placed above the antennas is used to reduce mutual coupling of the antenna array coupled in the E-plane. The initial antenna array without the metasurface is analyzed as a reference antenna. Fig. 20 indicates that the decoupled antenna array can achieve an isolation improvement of about 15 dB in the operating band (3.3–3.7 GHz) when it is well matched.

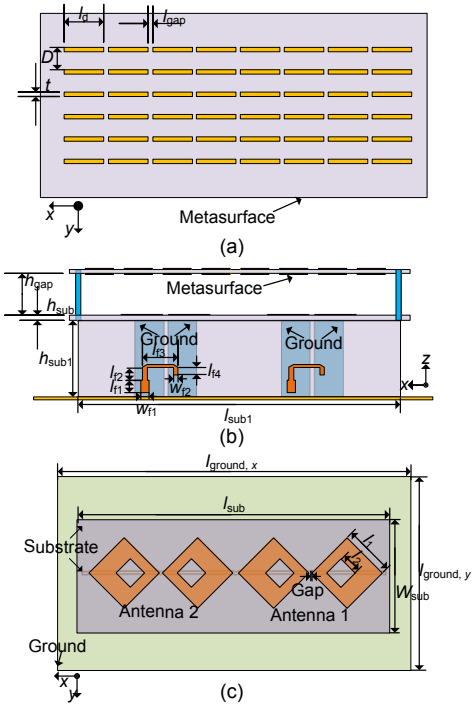

Fig. 19 Top view of the metasurface (a), side view of two square ring-shaped dipole (SRD) antennas (b), and top view of the two SRD antennas (c)
Reprinted from Guo et al. (2019), Copyright 2019, with permission from IEEE

Fig. 21 depicts the measured radiation patterns of the antenna arrays coupled and decoupled at 3.5 GHz. It can be seen that the gain of the antenna at the boresight improves by 1.5 dB after the metasurface is loaded compared with the antenna without metasurface, which can reach 7.2 dBi. Moreover, compared with the antenna before decoupling, the decoupled antenna's overall efficiency increases by about 5%, and the ECC reduces in the operating band (Fig. 22).

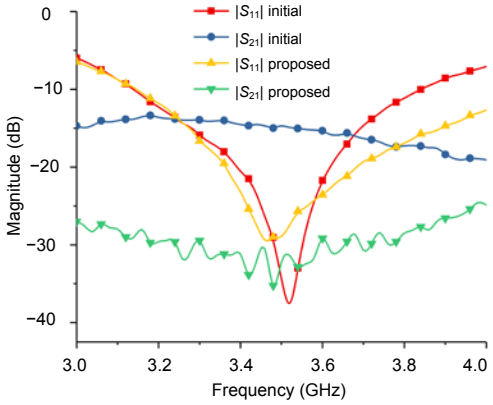

Fig. 20 Measured *S* parameters of antenna arrays with and without metasurface
Reprinted from Guo et al. (2019), Copyright 2019, with permission from IEEE

4 Conclusions

Multiple-input multiple-output (MIMO) technology plays an extremely important role in improving spectrum use and data transmission reliability. Moreover, for MIMO antenna systems, high isolation and miniaturization have become inevitable trends. However, port isolation and miniaturization have always constrained each other for multiple antennas. Since the mutual coupling between antenna elements deteriorates the array antenna's radiation performance and changes the radiation patterns, the array's mutual coupling affection is a problem that must be considered in the antenna array design. We have classified and analyzed the methods of mutual coupling reduction introduced in recent works, which is used as a basis for the novel work on antenna array decoupling. Results showed that the proposed decoupling method suppresses the mutual coupling of antennas arranged along not only the H-plane, but also the E-plane, which ensures good decoupling performance.

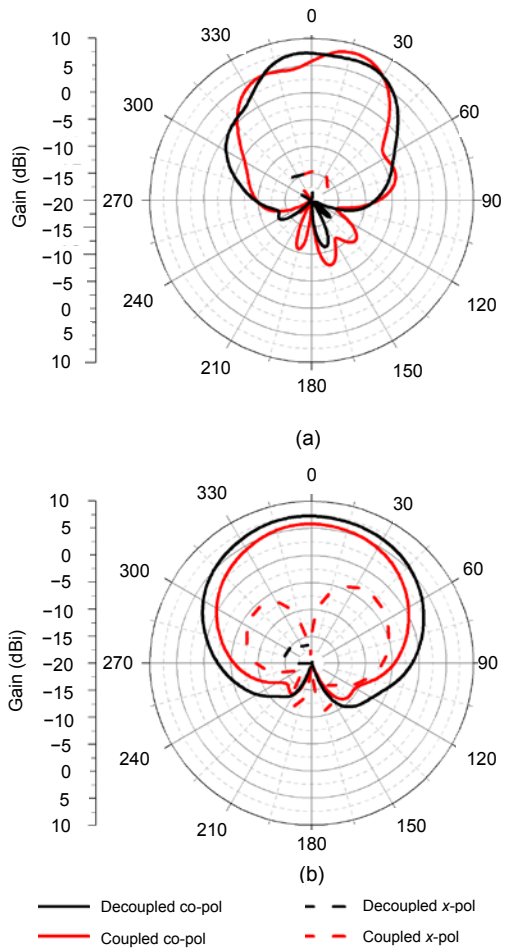

Fig. 21 Measured radiation patterns of antenna arrays at 3.5 GHz: (a) *xoz* plane; (b) *yoz* plane

Reprinted from Guo et al. (2019), Copyright 2019, with permission from IEEE

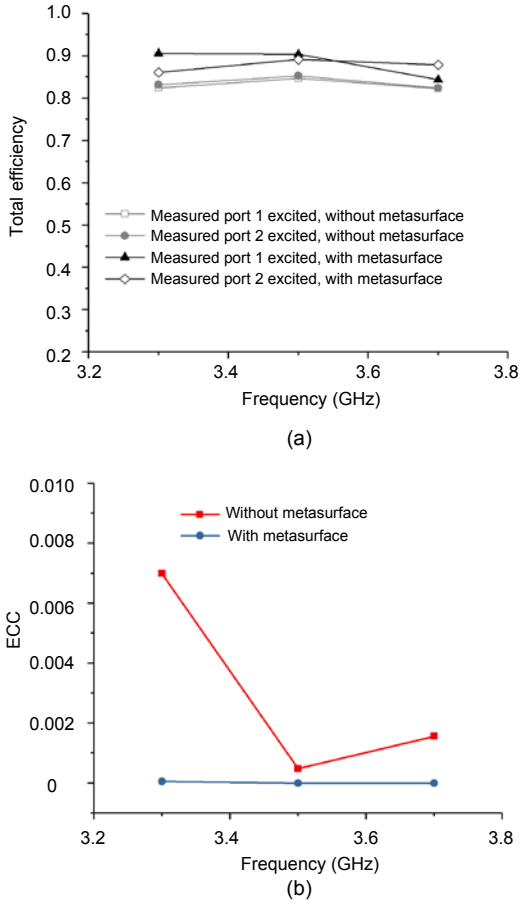

Fig. 22 Total measured efficiencies (a) and calculated envelope correlation coefficient (ECC) (b) of two antenna arrays coupled in the E-plane without and with metasurface

Reprinted from Guo et al. (2019), Copyright 2019, with permission from IEEE

Contributors

Jia-yin GUO designed the research. Lu-yu ZHAO guided the research. Feng LIU and Guo-dong JING processed the data. Jia-yin GUO and Feng LIU drafted the manuscript. Lu-yu ZHAO, Ying-zeng YIN, and Guan-long HUANG revised the manuscript. Jia-yin GUO finalized the paper.

Compliance with ethics guidelines

Jia-yin GUO, Feng LIU, Guo-dong JING, Lu-yu ZHAO, Ying-zeng YIN, and Guan-long HUANG declare that they have no conflict of interest.

References

Akbari M, Ghalyon HA, Farahani M, et al., 2017. Spatially decoupling of CP antennas based on FSS for 30 GHz MIMO systems. *IEEE Access*, 5:6527-6537. https://doi.org/10.1109/ACCESS.2017.2693342

Al-Hasan MJ, Denidni TA, Sebak AR, 2015. Millimeter-wave compact EBG structure for mutual coupling reduction applications. *IEEE Trans Antenn Propag*, 63(2):823-828. https://doi.org/10.1109/TAP.2014.2381229

Amjadi SM, Sarabandi K, 2016. Mutual coupling mitigation in broadband multiple-antenna communication systems using feedforward technique. *IEEE Trans Antenn Propag*, 64(5):1642-1652. https://doi.org/10.1109/TAP.2016.2535101

Browne DW, Manteghi M, Fitz MP, et al., 2006. Experiments with compact antenna arrays for MIMO radio communications. *IEEE Trans Antenn Propag*, 54(11):3239-3250. https://doi.org/10.1109/TAP.2006.883973

Chae SH, Oh Sk, Park SO, 2007. Analysis of mutual coupling, correlations, and TARC in WiBro MIMO array antenna. *IEEE Antenn Wirel Propag Lett*, 6:122-125. https://doi.org/10.1109/LAWP.2007.893109

Chen SC, Wang YS, Chung SJ, 2008. A decoupling technique for increasing the port isolation between two strongly coupled antennas. *IEEE Trans Antenn Propag*, 56(12):3650-3658. https://doi.org/10.1109/TAP.2008.2005469

Chiu CY, Cheng CH, Murch RD, et al., 2007. Reduction of mutual coupling between closely-packed antenna elements. *IEEE Trans Antenn Propag*, 55(6):1732-1738. https://doi.org/10.1109/TAP.2007.898618

Chiu CY, Xu F, Shen SP, et al., 2018. Mutual coupling reduction of rotationally symmetric multiport antennas. *IEEE Trans Antenn Propag*, 66(10):5013-5021. https://doi.org/10.1109/TAP.2018.2854301

Dhevi BL, Vishvaksenan KS, Rajakani K, 2018. Isolation enhancement in dual-band microstrip antenna array using asymmetric loop resonator. *IEEE Antenn Wirel Propag Lett*, 17(2):238-241. https://doi.org/10.1109/LAWP.2017.2781907

Ding CF, Zhang XY, Xue CD, et al., 2018. Novel pattern-diversity-based decoupling method and its application to multielement MIMO antenna. *IEEE Trans Antenn Propag*, 66(10):4976-4985. https://doi.org/10.1109/TAP.2018.2851380

Farahani M, Pourahmadazar J, Akbari M, et al., 2017. Mutual coupling reduction in millimeter-wave MIMO antenna array using a metamaterial polarization-rotator wall. *IEEE Antenn Wirel Propag Lett*, 16:2324-2327. https://doi.org/10.1109/LAWP.2017.2717404

Feng DQ, Jiang CZ, Lim GB, et al., 2013. A survey of energy-efficient wireless communications. *IEEE Commun Surv Tutor*, 15(1):167-178. https://doi.org/10.1109/SURV.2012.020212.00049

Getu BN, Andersen JB, 2005. The MIMO cube—a compact MIMO antenna. *IEEE Trans Wirel Commun*, 4(3):1136-1141. https://doi.org/10.1109/TWC.2005.846997

Guo JY, Liu F, Zhao LY, et al., 2019. Meta-surface antenna array decoupling designs for two linear polarized antennas coupled in H-plane and E-plane. *IEEE Access*, 7:100442-100452. https://doi.org/10.1109/ACCESS.2019.2930687

Jafri SI, Brown AK, Shafique MF, et al., 2016. Compact reconfigurable multiple-input-multiple-output antenna for ultra wideband applications. *IET Microw Antenn Propag*, 10(4):413-419. https://doi.org/10.1049/iet-map.2015.0181

Larsson EG, Edfors O, Tufvesson F, et al., 2014. Massive MIMO for next generation wireless systems. *IEEE Commun Mag*, 52(2):186-195. https://doi.org/10.1109/MCOM.2014.6736761

Lee JY, Kim SH, Jang JH, 2015. Reduction of mutual coupling in planar multiple antenna by using 1-D EBG and SRR structures. *IEEE Trans Antenn Propag*, 63(9):4194-4198. https://doi.org/10.1109/TAP.2015.2447052

Li JF, Chu QX, Li ZH, et al., 2013. Compact dual band-notched UWB MIMO antenna with high isolation. *IEEE Trans Antenn Propag*, 61(9):4759-4766. https://doi.org/10.1109/TAP.2013.2267653

Li Q, Feresidis AP, Mavridou M, et al., 2015. Miniaturized double-layer EBG structures for broadband mutual coupling reduction between UWB monopoles. *IEEE Trans Antenn Propag*, 63(3):1168-1171. https://doi.org/10.1109/TAP.2014.2387871

Li ZY, Du ZW, Takahashi M, et al., 2012. Reducing mutual coupling of MIMO antennas with parasitic elements for mobile terminals. *IEEE Trans Antenn Propag*, 60(2):473-481. https://doi.org/10.1109/TAP.2011.2173432

Liang PY, Wu Q, 2018. Characteristic mode analysis of antenna mutual coupling in the near field. *IEEE Trans Antenn Propag*, 66(7):3757-3762. https://doi.org/10.1109/TAP.2018.2823867

Liu F, Guo JY, Zhao LY, et al., 2018. A meta-surface decoupling method for two linear polarized antenna array in sub-6 GHz base station applications. *IEEE Access*, 7:2759-2768. https://doi.org/10.1109/ACCESS.2018.2886641

Ouyang J, Yang F, Wang ZM, 2011. Reducing mutual coupling of closely spaced microstrip MIMO antennas for WLAN application. *IEEE Antenn Wirel Propag Lett*, 10:310-313. https://doi.org/10.1109/LAWP.2011.2140310

Pan BC, Cui TJ, 2017. Broadband decoupling network for dual-band microstrip patch antennas. *IEEE Trans Antenn Propag*, 65(10):5595-5598. https://doi.org/10.1109/TAP.2017.2742539

Soltani S, Murch RD, 2015. A compact planar printed MIMO antenna design. *IEEE Trans Antenn Propag*, 63(3):1140-1149. https://doi.org/10.1109/TAP.2015.2389242

Su SW, Lee CT, Chang FS, 2012. Printed MIMO-antenna system using neutralization-line technique for wireless USB-dongle applications. *IEEE Trans Antenn Propag*, 60(2):456-463. https://doi.org/10.1109/TAP.2011.2173450

Sun HH, Ding C, Zhu H, et al., 2019. Suppression of cross-band scattering in multiband antenna arrays. *IEEE Trans Antenn Propag*, 67(4):2379-2389. https://doi.org/10.1109/TAP.2019.2891707

Tang MC, Chen ZY, Wang H, et al., 2017. Mutual coupling reduction using meta-structures for wideband, dual-polarized, and high-density patch arrays. *IEEE Trans Antenn Propag*, 65(8):3986-3998. https://doi.org/10.1109/TAP.2017.2710214

Wang ZY, Zhao LY, Cai YM, et al., 2018. A meta-surface antenna array decoupling (MAAD) method for mutual coupling reduction in a MIMO antenna system. *Sci Rep*, 8:3152. https://doi.org/10.1038/s41598-018-21619-z

Wei K, Li JY, Wang L, et al., 2016. Mutual coupling reduction by novel fractal defected ground structure band-gap filter. *IEEE Trans Antenn Propag*, 64(10):4328-4335. https://doi.org/10.1109/TAP.2016.2591058

Wu KL, Wei CW, Mei XD, et al., 2017. Array-antenna decoupling surface. *IEEE Trans Antenn Propag*, 65(12):6728-6738. https://doi.org/10.1109/TAP.2017.2712818

Xue CD, Zhang XY, Cao YF, et al., 2017. MIMO antenna using hybrid electric and magnetic coupling for isolation enhancement. *IEEE Trans Antenn Propag*, 65(10):5162-5170. https://doi.org/10.1109/TAP.2017.2738033

Yang F, Rahmat-Samii Y, 2003. Microstrip antennas integrated with electromagnetic band-gap (EBG) structures: a low

mutual coupling design for array applications. *IEEE Trans Antenn Propag*, 51(10):2936-2946. https://doi.org/10.1109/TAP.2003.817983

Zhai GH, Chen ZN, Qing XM, 2016. Mutual coupling reduction of a closely spaced four-element MIMO antenna system using discrete mushrooms. *IEEE Trans Microw Theory Technol*, 64(10):3060-3067. https://doi.org/10.1109/TMTT.2016.2604314

Zhang S, Pedersen GF, 2016. Mutual coupling reduction for UWB MIMO antennas with a wideband neutralization line. *IEEE Antenn Wirel Propag Lett*, 15:166-169. https://doi.org/10.1109/LAWP.2015.2435992

Zhang S, Lau BK, Tan Y, et al., 2012. Mutual coupling reduction of two PIFAs with a T-shape slot impedance transformer for MIMO mobile terminals. *IEEE Trans Antenn Propag*, 60(3):1521-1531. https://doi.org/10.1109/TAP.2011.2180329

Zhang Y, Zhang XY, Ye LH, et al., 2016. Dual-band base station array using filtering antenna elements for mutual coupling suppression. *IEEE Trans Antenn Propag*, 64(8): 3423-3430. https://doi.org/10.1109/TAP.2016.2574872

Zhao LY, Wu KL, 2014. A decoupling technique for four-element symmetric arrays with reactively loaded dummy elements. *IEEE Trans Antenn Propag*, 62(8):4416-4421. https://doi.org/10.1109/TAP.2014.2326425

Zhao LY, Wu KL, 2015. A dual-band coupled resonator decoupling network for two coupled antennas. *IEEE Trans Antenn Propag*, 63(7):2843-2850. https://doi.org/10.1109/TAP.2015.2421973

Zhao LY, Yeung LK, Wu KL, 2014. A coupled resonator decoupling network for two-element compact antenna arrays in mobile terminals. *IEEE Trans Antenn Propag*, 62(5):2767-2776. https://doi.org/10.1109/TAP.2014.2308547

Zhao X, Yeo SP, Ong LC, 2018. Decoupling of inverted-F antennas with high-order modes of ground plane for 5G mobile MIMO platform. *IEEE Trans Antenn Propag*, 66(9):4485-4495. https://doi.org/10.1109/TAP.2018.2851381

Zhu YF, Chen YK, Yang SW, 2019. Decoupling and low-profile design of dual-band dual-polarized base station antennas using frequency-selective surface. *IEEE Trans Antenn Propag*, 67(8):5272-5281. https://doi.org/10.1109/TAP.2019.2916730